28. Materials and methods are available as supplementary materials on *Science* Online.
29. R. A. Bagnold, *The Physics of Blown Sand and Desert Dunes* (Dover Publications, Mineola, NY, 2005).
30. G. Cho, J. Dodds, J. C. Santamarina, *J. Geotech. Geoenviron. Eng.* **132**, 591 (2006).
31. B. Chaudhuri, A. Mehrotra, F. J. Muzzio, M. S. Tomassone, *Powder Technol.* **165**, 105 (2006).
32. K. Kamrin, G. Koval, *Phys. Rev. Lett.* **108**, 178301 (2012).
33. J. A. Clack, *Gaining Ground: The Origin and Evolution of Tetrapods* (Indiana Univ. Press, Bloomington, IN, 2012).

Acknowledgments: We thank Y. Ding, P. Umbanhowar, N. Gravish, G. Meirion-Griffith, S. Sharpe, H. Komsuoglu, D. Koditschek, and R. Full for discussions; J. Shen for assistance with robot modification; P. Masarati for multibody dynamic simulator support; S. Sharpe for measuring the angle of repose of 3-mm glass spheres and assistance with photography; P. Umbanhowar and H. Marvi for natural sand collection; and all the members of the Complex Rheology And Biomechanics Lab at Georgia Tech for general assistance. This work was supported by the Burroughs Wellcome Fund, the Army Research Laboratory Micro Autonomous Systems and Technology Collaborative Technology Alliance, the Army Research Office, and the NSF Physics of Living Systems program. C.L. was partially supported by a Miller Research Fellowship from the Miller Institute for Basic Research in Science of the University of California, Berkeley. The authors declare that they have no competing interests. C.L. designed the study, performed resistive force measurements, and performed robot experiments; C.L. and T.Z. performed model calculations; T.Z. performed robot simulation; D.I.G. oversaw the study; and C.L. and D.I.G. wrote the paper.

Supplementary Materials

www.sciencemag.org/cgi/content/full/339/6126/1408/DC1
Materials and Methods
Supplementary Text
Figs. S1 to S14
Tables S1 to S4
References (*34*–*38*)
Movies S1 to S6
Additional Data Table S5

22 August 2012; accepted 15 January 2013
10.1126/science.1229163

DNA Gridiron Nanostructures Based on Four-Arm Junctions

Dongran Han,[1,2]* Suchetan Pal,[1,2] Yang Yang,[1,2] Shuoxing Jiang,[1,2] Jeanette Nangreave,[1,2] Yan Liu,[1,2]* Hao Yan[1,2]*

Engineering wireframe architectures and scaffolds of increasing complexity is one of the important challenges in nanotechnology. We present a design strategy to create gridiron-like DNA structures. A series of four-arm junctions are used as vertices within a network of double-helical DNA fragments. Deliberate distortion of the junctions from their most relaxed conformations ensures that a scaffold strand can traverse through individual vertices in multiple directions. DNA gridirons were assembled, ranging from two-dimensional arrays with reconfigurability to multilayer and three-dimensional structures and curved objects.

Self-assembling nucleic acid molecules have shown merit as versatile materials for organizing and constructing complex nanoscale structures (*1*). In 2006, Rothemund described a method to generate complex DNA origami nanostructures with addressable surface features. In this method, a long scaffold strand, most often the 7429-nucleotide (nt) circular genome of the M13mp18 bacteriophage, is organized and folded by interactions with a large number of short, synthetic, staple strands (*2*). The path of the scaffold strand in this approach has been restricted to discrete domains of parallel lines because it is based on the double crossover unit motif to link adjacent helices (*3*–*5*). We present a design strategy that uses an unusual set of immobile Holliday junction analogs (four-arm junctions) as the basic structural unit of DNA origami nanostructures and as joints to construct a variety of two-dimensional (2D) and 3D gridiron structures, in which the scaffold strand and corresponding double helices are not restricted to a 1D parallel, raster-fill pattern. By programming the connection between individual joints with DNA segments of variable lengths, we constructed complex wireframe geometries.

Although intuitively one could imagine threading a single-stranded scaffold through a number of four-arm junction units in both horizontal and vertical directions to create gridiron like patterns, the structural properties of traditional Holliday junction (*6*–*8*) impose certain challenges that require unconventional rearrangement of the junction unit conformation, as revealed by the design principles described below. We compared a gridiron unit to a double crossover motif (*9*) (Fig. 1A), and the DNA strands are abstracted to display only their polarity with the arrows pointing from 5′ to 3′. In the gridiron unit, four four-arm junctions are linked together to form a two-layer square frame in which the helices on opposite sides lie in the same plane. An antiparallel arrangement between opposite sides of the square frame permits a single, central strand to traverse each of the helices.

Each of the four junctions is depicted in its relaxed conformation (Fig. 1B) such that the helices form a right-handed twist with a 60° torsion angle. Deviation from a relaxed conformation is required of each junction to form the gridiron unit cell. First, the red strands in the horizontally oriented helices (both top and bottom images) can be linked together to produce continuous strands without reversing the 5′-to-3′ polarity (Fig. 1, B and C). Next, the vertically oriented helices need to be rotated in the plane about the junction points (Fig. 1C) to allow the formation of continuous 5′-to-3′ connections between upper and lower junctions (Fig. 1, D and E).

Connecting a number of gridiron units leads to the formation of a variety of 2D lattices (Fig. 1, F and G). The red lines represent the DNA strands that are expected to retain an unperturbed helical structure with continuous base stacking. Meanwhile, the short strands (in gray) form the crossovers between helical domains and function as staples. A long scaffold strand is created by connecting the termini of the red strands with short single-stranded DNA (ssDNA) loops. In the most basic design, the scaffold begins at one corner, fills the first layer, changes direction at the opposite corner, and then fills the second layer to produce a structure in which the helices within the two layers are oriented perpendicularly with respect to each other. Lastly, the scaffold returns to its initial position to form a closed loop (Fig. 1G).

The cavity size of gridiron structures can be tailored by altering the number of base pairs between the adjacent junction points. An 11-by-11 gridiron structure (11 vertical helices by 11 horizontal helices) with 21 base pairs (bp) between junctions in both directions uses 5301 of 7249 nt of the M13mp18 ssDNA scaffold strand and contains 120 staple strands (42 nt each). The remaining 1948 nt of the scaffold form a single-stranded loop at one corner that is visible in atomic force microscope (AFM, Fig. 2, A and B) and transmission electron microscope (TEM) images (Fig. 2, C and D). Gridiron structures with 63-by-63–bp cavities (Fig. 2, E and F) were assembled to demonstrate the programmability of the design strategy.

To test whether the ssDNA scaffold is required to force the junction to rotate and form the intended gridiron structures, we designed and successfully constructed a scaffold-free 11-by-11 gridiron structure (figs. S13 and S14). We also found that scaffolded and scaffold-free gridiron elements can be combined within a single structure (figs. S13 and S15). Further, a scaffold-free gridiron unit was examined by native gel electrophoresis to verify its formation when the component strands were mixed in equal stoichiometric ratios (fig. S33). Although the schematic diagram in Fig. 1D depicts 90° angles between the helices in the upper and lower layers, the angles are not fixed because the junctions are flexible. The experimental results reveal the formation of rhomboid rather than square structures; the junctions most likely behave cooperatively in order to maintain optimized base-stacking interactions and the lowest overall free energy. The single-stranded

[1]The Biodesign Institute, Arizona State University, Tempe, AZ 85287, USA. [2]Department of Chemistry and Biochemistry, Arizona State University, Tempe, AZ 85287, USA.

*Corresponding author. E-mail: hao.yan@asu (H.Y.); yan_liu@asu.edu (Y.L.); dongran.han@asu.edu (D.H.)

Downloaded from http://science.sciencemag.org/ on May 7, 2018

scaffold loop in one corner serves as an intrinsic marker to determine the angles adopted by the gridiron, and the angles display a bimodal distribution with nearly equal amplitudes, centered at 76° ± 7° (SD) and 103° ± 7° (for additional details regarding image analysis, see fig. S7). A closer examination of the AFM images further reveals the existence of two alternative conformations that the structural can adopt (figs. S6 and S8 and discussion in supplementary text).

The flexibility of the joints makes it possible to control or reconfigure the conformation of the gridiron structure by exerting external forces on selected corners of a gridiron. A modified version of a 15-by-15 gridiron structure with 21-bp cavities has about one quadrant of the gridiron unfolded and forms a randomly coiled 836-nt single-stranded loop between two "arms" of tweezers (Fig. 2G). The ssDNA loop is long enough to allow the structure to adopt a relaxed conformation. The observed distribution of the inner angle (θ) of the tweezers (measured from 309 individual structures) is broad and centered at 80° to 90°.

We could contract and extend the ssDNA loop by introducing secondary or tertiary structures that generate enough force to control the angle (the design details are described in the supplementary materials). Sets of staple strands were designed to either contract the ssDNA loop and fix an acute angle (a narrow distribution centered at 41° ± 7°) via the formation of a two-helix bundle (Fig. 2H) or to extend the loop to secure a right (Fig. 2I) or obtuse angle (Fig. 2J) via the formation of a three-helix bundle of specific length. The design with the right angle shows a narrow and symmetrical distribution centered at 94° ± 10°, and the design with the obtuse angle has a broader angle distribution centered at 102° and exhibits an asymmetry that is more heavily weighted toward smaller angles.

We extended the gridiron design into the third dimension by three different strategies. The first involves stacking multiple layers of 2D gridiron lattices at selected connection points (Fig. 3, A and B). The second relies on intertwining several gridiron planes in *x*-*y*-*z* directions (Fig. 3C). The third method has its basis in distorting a single layer of DNA gridiron into 3D structures by controlling their curvatures (Fig. 4). By using the first strategy, we constructed a three-layer hexagonal (Fig. 3D), a four-layer rectangular gridiron (Fig. 3E), and a three-layer parallelogram (fig. S58) structure. For all multilayer gridiron structures, the scaffold strand raster fills each layer, with an offset in the angle formed between the helices of adjacent layers. The three-layer hexagonal and four-layer rectangular structures maintained 60° and 90° offsets between layers, respectively.

Varying the location and distance between connection points will yield differently patterned multilayer structures. In contrast to the angle flexibility present in the quasi-2D structures, the addition of a third layer fixes the angles at junction points. The only exception to this is for connections through the center of the same unit motif, as shown by the green dashed line (Fig. 3A). In a 3D model of an eight-by-eight-by-eight three-layer hexagonal gridiron structure (Fig. 3D), neighboring junctions in the top and bottom layers are 52 bp apart, and neighboring junctions in the middle layer (alternating connections to the top and bottom layers) are 26 bp apart. Because $X = Y = L$ (Fig. 3B), each junction should adopt a 60° torsion angle. A four-layer rectangular gridiron structure (Fig. 3E) can be broken down into two six-by-five double-layer gridirons (with 52-bp cavities) stacked on top of one another with a 26-bp offset in the connections between the first and third, and second and fourth, layers.

The relations of the lattice planes in gridiron structures are not restricted to stacked multilayer structures. The 3D gridiron structures can also be assembled by integrating gridiron lattices with scaffold-free elements (see supplementary materials for description of various design possibilities). Figure 3F presents such a design in which a nine-by-nine gridiron plane (shown in blue) is intertwined with an eight-by-eight scaffold-free gridiron plane (shown in yellow). The complex, interwoven topology of this particular structure required combining scaffolded and scaffold-free components (see supplementary materials for additional details).

Gridiron designs can allow assembly of even more complex structures by inducing a desired curvature in the basic structural unit described in Fig. 1. Maintaining the distance between junctions in one direction while simultaneously shrinking or extending the distance in the other direction (by varying the number of base pairs) creates an isosceles trapezoid unit. The lengths of the parallel sides of the trapezoidal units can be progressively changed between layers and combined to generate curved gridiron structures such as an S-shaped structure (Fig. 4A). One layer is composed of nine concentric, evenly spaced curved helices, and the second layer contains 13 linear,

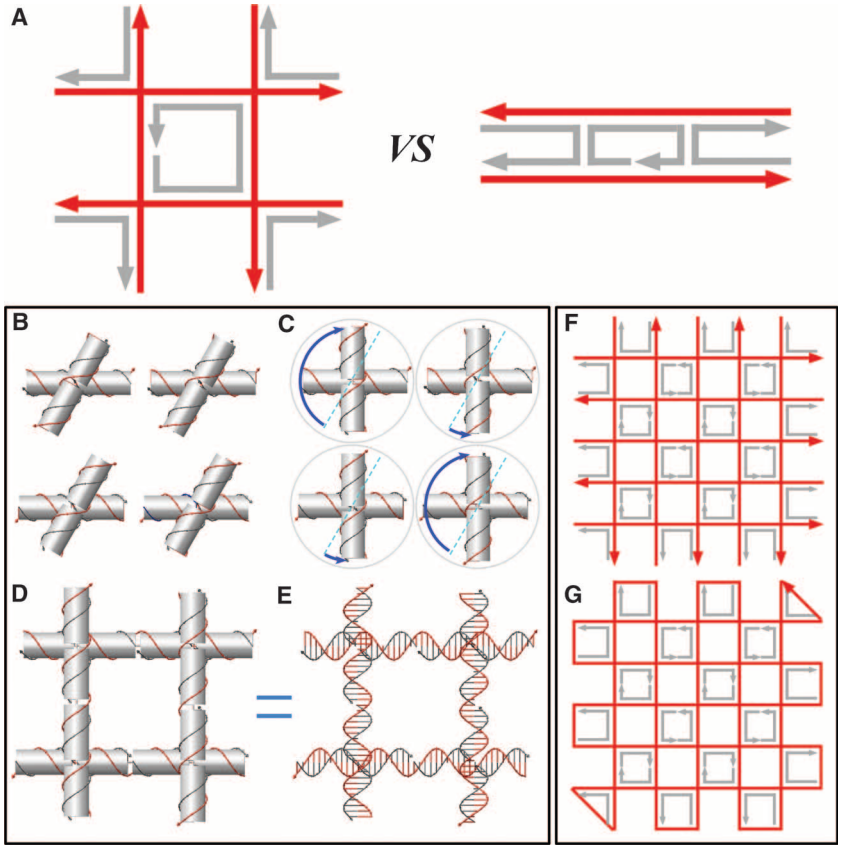

Fig. 1. (**A**) (Left) Geometry and strand polarity of a single gridiron unit formed from four four-arm junctions. (Right) Geometry and polarity of a double-crossover molecule motif used in conventional DNA origami structures. For both structures, the ssDNAs depicted in red are components of DNA double helices that serve as the scaffold strands. The ssDNA depicted in gray represents staple strands. (**B**) Models of four four-arm junction molecules in their relaxed conformation. The orientation of the upper two junctions differs from that of the lower two by a 180° in-plane rotation. Thus, the polarities of the continuous red strands in the upper and lower layers of the horizontally oriented helices are antiparallel to one another. (**C**) Models illustrating the deviation from a relaxed conformation required of the four individual junctions to form a gridiron unit. The blue arrows indicate that the top helix of the junctions in the upper-left and lower-right corners must be rotated ~150° clockwise, whereas in the upper-right and lower-left junctions they must be rotated ~30° counterclockwise. (**D** and **E**) Helical models illustrating a complete gridiron unit. (**F** and **G**) Schematics illustrating a typical scaffold-folding path for a 2D DNA gridiron pattern.

Downloaded from http://science.sciencemag.org/ on May 7, 2018

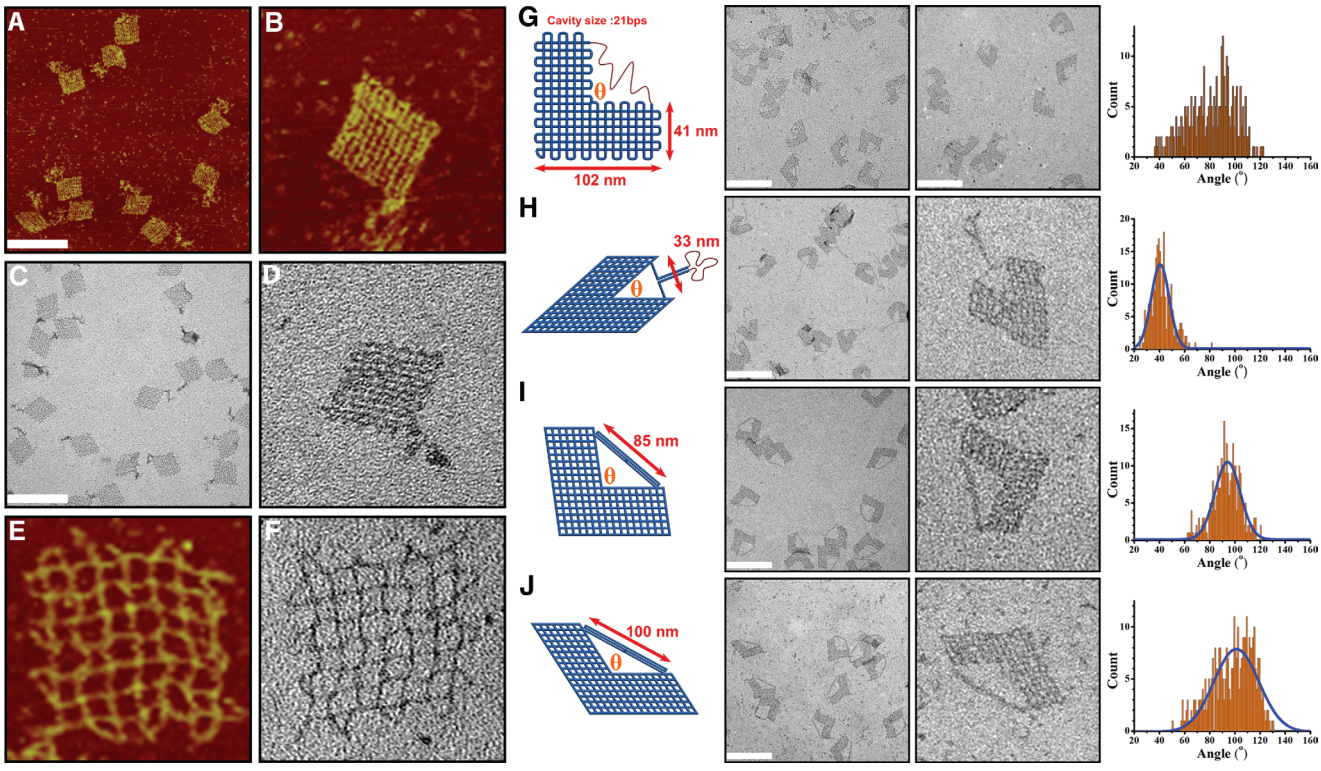

Fig. 2. (**A** to **D**) Images for a 2D gridiron structures with 21-bp cavities with AFM [(A) and (B)] and TEM images [(C) and (D)]. (**E** and **F**) Images for a 2D gridiron with 63-bp cavities with AFM (E) and TEM images (F). (**G** to **J**) Schematics (left), TEM images (middle), and histogram analysis (right) of the angle distributions for angle control. All scale bars indicate 200 nm, and all zoom-in images (images without scale bars) are 200 by 200 nm.

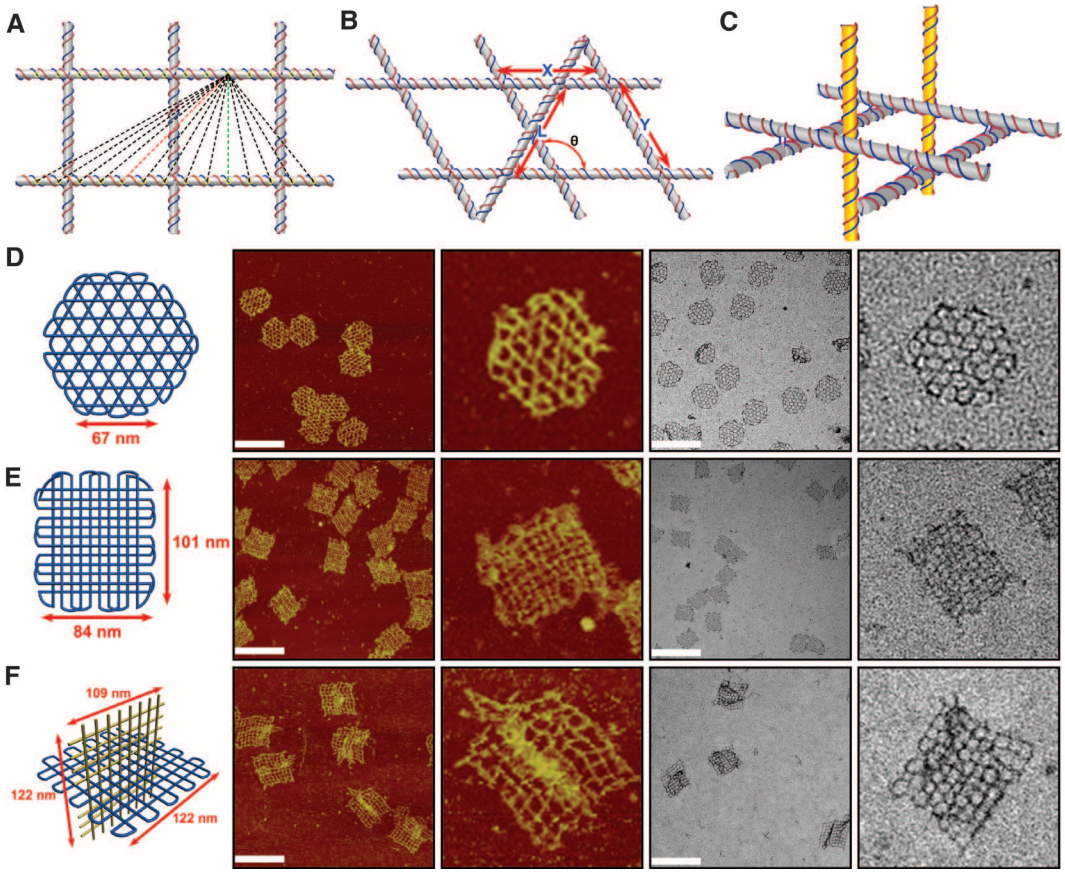

Fig. 3. Multilayer gridiron design strategies. (**A** and **B**) Strategy 1 is stacked layers. (A) A portion of a double-layer gridiron lattice with 52-bp cavity size. The yellow circles designate the permissible connection points to a third layer. The dashed lines correspond to possible connection points to form additional layers. (B) Given the double-layer gridiron lattice (*X* and *Y* lengths) and the distance between crossover points in the third layer, the angle θ can be calculated as $180° - \cos^{-1}[(X^2 + Y^2 - L^2)/2XY]$. (**C**) Strategy 2 is intertwining gridiron planes. (**D** to **F**) Schematics (left), AFM (middle), and TEM (right) images of (D) a three-layer hexagonal gridiron design, θ = 120°; (E) a four-layer gridiron design, θ is not controlled because the dashed green line in (A) represents a connection strategy that cannot fix the angle; and (F) a 3D gridiron assembled by using strategy 2. All scale bars indicate 200 nm, and all zoom-in images (images without scale bars) are 200 by 200 nm.

Downloaded from http://science.sciencemag.org/ on May 7, 2018

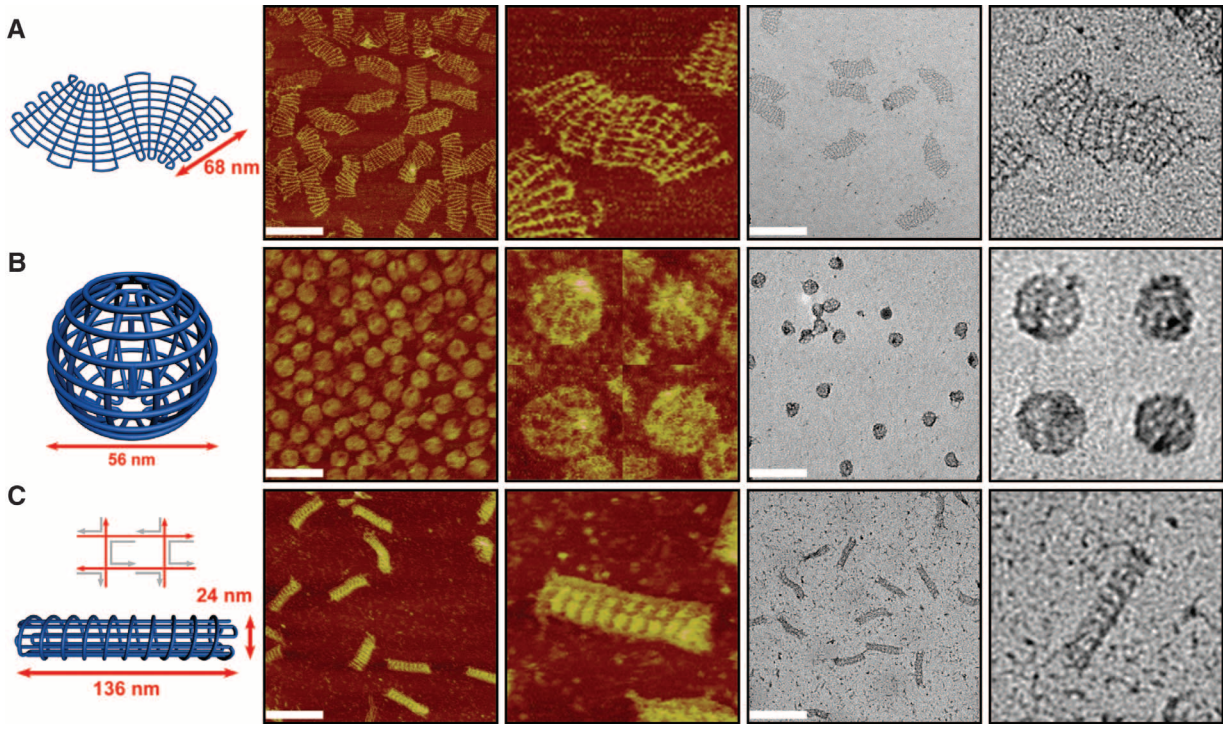

Fig. 4. Schematics (left), AFM (middle), and TEM images (right) of (**A**) an S-shaped structure, (**B**) a sphere, and (**C**) a screw. All scale bars indicate 200 nm, and all zoom-in images (images without scale bars) are 200 by 200 nm. In (B) and (C), the diameter and the width, respectively, appear to be larger in the AFM images compared with the TEM images. This difference is probably a result of flattening of the 3D objects into two-layer structures and AFM tip convolution.

nonparallel helices. The relation between adjacent linear helices (the angles formed by their theoretical intersection) between adjacent linear helices was varied. Some 3D gridiron structures that contain curvature were also achieved, such as the sphere shown in Fig. 4B. The helices in concentric ring and radial spoke layers are stretched in the center and shrunk at the edges, forming a latitudinal and longitudinal framework, respectively. This is realized by progressively adjusting the distance between junctions in latitudinal directions. Additional modifications to the basic structural motif can be used to produce other complex structures. In the screw structure (Fig. 4C), the polarity of the DNA strands in the square unit motif differs from what is illustrated in Fig. 1B (where adjacent scaffold helices have an antiparallel polarity in one direction and the same polarity in the other direction). The scaffold strand is arranged in an antiparallel configuration to form a wireframe cylinder structure (11 helices are arranged axially) and subsequently wraps around the cylinder (analogous to a left-handed screw) until the two ends meet. The distance between adjacent axial helices is 21 bp, the interthread distance is 42 bp, and the AFM and TEM images display the expected left-handed conformation.

The design principles of creating gridiron units allow scaffold strands to travel in multiple directions, which represent an important departure from certain aspects of the previous DNA origami methods. Traditional Holliday junctions do not naturally adopt conformations that would allow them to be connected in such a way, and it was unexpected to find that these motifs could (within a larger network of crossovers) endure a 150° rotation of one of the arms while simultaneously maintaining their integrity. Indeed, the flexible and dynamic behavior of these motifs may have excluded these types of junction conformations for consideration in scaffolded structures. Yield analysis from agarose gel and TEM images shows that the structures, even without purification, form with reasonably high yield (from ~36% for the gridiron tweezers to ~85% for the gridiron screw, estimated from agarose gels; from ~51% for the gridiron sphere to ~89% for the four-layer gridiron, estimated from TEM images; see supplementary materials for yield analysis). The ability to engineer DNA gridirons that are analogous to vector-based objects, where a series of points with defined positions in 3D space are connected by lines, is an important milestone in the development of synthetic nucleic acid structures. In particular, this opens up new opportunities to implement the design of complex wireframe structures (see discussion in supplementary materials) that are amenable to dynamic controls. A future challenge in DNA origami is to achieve true folding, starting from a 2D sheet (miura ori), rather than the 1D M13 scaffolds commonly used in traditional DNA origami construction. The loose 2D networks and freely rotating hinges between different planes of DNA gridirons provide the design features necessary to implement Miura ori type of origami.

References and Notes

1. N. C. Seeman, *Annu. Rev. Biochem.* **79**, 65 (2010).
2. P. W. K. Rothemund, *Nature* **440**, 297 (2006).
3. S. M. Douglas *et al.*, *Nature* **459**, 414 (2009).
4. H. Dietz, S. M. Douglas, W. M. Shih, *Science* **325**, 725 (2009).
5. D. Han *et al.*, *Science* **332**, 342 (2011).
6. C. Mao, W. Sun, N. C. Seeman, *J. Am. Chem. Soc.* **121**, 5437 (1999).
7. S. M. Miick, R. S. Fee, D. P. Millar, W. J. Chazin, *Proc. Natl. Acad. Sci. U.S.A.* **94**, 9080 (1997).
8. S. A. McKinney, A. C. Déclais, D. M. J. Lilley, T. Ha, *Nat. Struct. Biol.* **10**, 93 (2002).
9. T. J. Fu, N. C. Seeman, *Biochemistry* **32**, 3211 (1993).

Acknowledgments: We thank N. Seeman and R. Sha from New York University for helpful discussions. This work is supported by NSF grant 1104373, Office of Naval Research grant N000140911118, Army Research Office grant W911NF-11-1-0137 to H.Y. and Y.L. and Army Research Office Multidisciplinary University Research Initiative award W911NF-12-1-0420 and National Science Foundation of China grant 21028005 to H.Y. H.Y. and Y.L. are part of the Center for Bio-Inspired Solar Fuel Production, an Energy Frontier Research Center funded by the U.S. Department of Energy, Office of Science, Office of Basic Energy Sciences under award no. DE-SC0001016. H.Y. is supported by the Presidential Strategic Initiative Fund from Arizona State University. The DNA sequences for the nanostructures and additional data described in this work can be found in the online supplementary materials.

Supplementary Materials

www.sciencemag.org/cgi/content/full/339/6126/1412/DC1
Materials and Methods
Supplementary Text
Figs. S1 to S96
Tables S1 to S17

1 November 2012; accepted 31 December 2012
10.1126/science.1232252

Downloaded from http://science.sciencemag.org/ on May 7, 2018

Science

DNA Gridiron Nanostructures Based on Four-Arm Junctions

Dongran Han, Suchetan Pal, Yang Yang, Shuoxing Jiang, Jeanette Nangreave, Yan Liu and Hao Yan

Science **339** (6126), 1412-1415.
DOI: 10.1126/science.1232252

Rewiring DNA Origami

Complex DNA nanostructures can be formed from a long scaffold strand of DNA by binding many shorter "staple" strands. In these DNA origami structures, the path of the scaffold has been restricted by a double-crossover motif to form parallel helices. **Han *et al.*** (p. 1412) now describe a more flexible approach based on a "gridiron unit" in which four four-arm junctions link together to form a two-layer square frame. A variety of two- and three-dimensional structures were created, including highly curved structures, such as a sphere and a screw.

ARTICLE TOOLS http://science.sciencemag.org/content/339/6126/1412

SUPPLEMENTARY MATERIALS http://science.sciencemag.org/content/suppl/2013/03/20/339.6126.1412.DC1

REFERENCES This article cites 9 articles, 3 of which you can access for free
http://science.sciencemag.org/content/339/6126/1412#BIBL

PERMISSIONS http://www.sciencemag.org/help/reprints-and-permissions

Use of this article is subject to the Terms of Service

Science (print ISSN 0036-8075; online ISSN 1095-9203) is published by the American Association for the Advancement of Science, 1200 New York Avenue NW, Washington, DC 20005. 2017 © The Authors, some rights reserved; exclusive licensee American Association for the Advancement of Science. No claim to original U.S. Government Works. The title *Science* is a registered trademark of AAAS.

Downloaded from http://science.sciencemag.org/ on May 7, 2018